Modeling of Electrical off-grid Network in the Simscape Power Systems

Dušan Medveď, Marián Klešč
Department of Electrical Power Engineering
Mäsiarska 74
042 00 Košice, Slovak Republic
dusan.medved@tuke.sk , Marian.Klesc@student.tuke.sk

Abstract — **This paper deals with the modeling and analysis of off-grid electrical networks. The library of Simscape Power Systems, part of the Simulink program, was used to model off-grid networks. The off-grid model includes electricity generation using diesel generators, photovoltaic panels and wind turbines, power consumption and basic electrical measurements. The impact of the different operating states on the modeled off-grid network has been analyzed, such as load coupling, load disconnection, load balancing, and changing of climatic conditions for photovoltaic panels and wind turbine.**

Keywords: off-grid network, Simscape Power Systems, diesel generator, photovoltaic panels, wind turbine

I. Introduction

This paper presents the results of the simulation of the impact of different electricity sources on a small off-grid. Diesel generators, photovoltaic fields and wind turbines have been used as power sources. From the point of view of electricity consumption, the effect of disconnection or connection of a large load on the system and the effect of a dynamically changing load is described. Multiple circuits have been simulated to verify some of the network phenomena. The main monitored variables included network frequency, voltage at the point of consumption, and power produced by sources.

To simulate these phenomena, the Simscape Power Systems, which is an extension of Matab Simulink, was used. Based on the simulation analysis, a simple solution was developed to reduce the impact of transient phenomena. Since simulated transient phenomena of a short nature, i.e. they take a short time, the designed simulations simulate the time interval within 1000 seconds, which is about 17 minutes. A short time interval has also been chosen because the results that are written in matrices have some accuracy and can be processed with current common computing techniques.

As a basis for these considerations, papers from engineers involved in the IEEE association, the world's largest technological advancing organization, have been used.

II. Description of the Network Model in the Environment of Simscape Power Systems

A. Power sources

In the Simscape Power Systems, several electrical machines are implemented. Many of these electric machines can work in two states – as electricity generators or as motors, that is, as electric consumer appliances [1], [2].

A model of the synchronous machine with expressed poles was used. The synchronous generator is controlled by a hydraulic turbine combined with the PID control system and excited by the AC4A excitation system. The principal scheme of the G1 generator with a control and exciter system and generating output from the generator can be seen in Fig. 1.

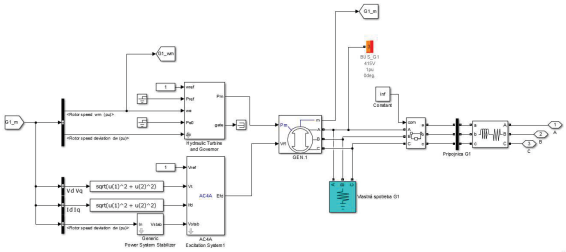

Figure 1. Principal scheme of the G1 generator connection

Output of the synchronous generator is a three-phase voltage at the terminals of the machine A, B and C and the measurement output marked with the letter m. The measurement output includes a vector with measured signals: stator currents, stator voltages, rotor angle deviation, rotor speed, electromagnetic torque, output active power P, output reactive power Q, and so on. These signals receive feedback from the generator that is input to the exciter winding input and the hydraulic turbine with the control. The label data of the simulated generator are shown in Tab. I.

Table 1. Data Of the Simulated Generator

		Reactances [pu]			
P_n	250 kW	x_d	2,84	x_q	2,44
V_n	415 V	$x_{d'}$	0,18	$x_{q'}$	0,36
f_n	50 Hz	$x_{d''}$	0,13	$x_{q''}$	0,09
Stator resistance R_s [pu]				0,0259375	
Coefficient of inertia H [s]				3,2	
Coefficient of friction F [pu]				0,01579	
Number of pole pairs p [–]				2	

In Fig. 2 is a model of a hydraulic turbine with PID control. This model has 5 inputs and 2 outputs. Inputs include reference speed, instantaneous mechanical speed, speed deviation, reference power and instantaneous power output. The output is the mechanical power P_m, which is also the input for the

synchronous generator. In the mentioned model was set the reference speed $\omega_{ef} = 1$ pu, and the inputs of the immediate mechanical velocity ω_e and the velocity variation $d\omega$ were connected. This regulation ensures the regulation of the synchronous generator at the nominal frequency $f_n = 50$ Hz. Inputs of the reference mechanical power P_{ref} and instantaneous power P_{e0} are not connected. The circuit is set so that it does not take any feedback (or feedback from the gate output). It has been achieved that the turbine power was controlled only by rotor speed [7].

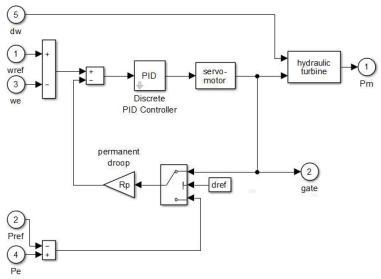

Figure 2. Hydraulic turbine diagram with PID control

As the excitation system, the AC4A excitation system was used, which is an excitation system with thyristor rectifier for AC alternator. The excitation system generates the excitation voltage that is the output of this model.

Generating power from the generator into the grid consists of a three-phase circuit breaker and a busbar measuring the terminal voltage and the supplied power to the grid. Behind these terminals there is a power line simulated by the resistance *R* and the inductance *L*. The mentioned generated power transmission into the output grid is shown in Fig. 1. Generator terminals are connected to the generator's own consumption, which consists of an active load of $P = 12.5$ kW. This load has been used because the synchronous generator simulated as a current source cannot be in series with the induction element of the three-phase line with which the generator is connected to the grid.

B. *Photovoltaic field*

Another source of electrical power that has been implemented in this paper is photovoltaic (PV) panels. The PV array is located in Simscape Power Systems block to simulate the photovoltaic panels. That's why the LG Electronics LG300N1-G3 photovoltaic panel has been selected. The label data of the modeled PV module are shown in Tab. II.

Table 2. Module Data for Photovoltaic Panel

Module data of PV array: LG Electronics LG300N1C-G3			
Max power [W]	305,226	Cell number in module (Ncell)	96
Open-circuit voltage V_{oc} [V]	64,2	Short-circuit current [A]	5,96
Voltage at max power V_{mp} [V]	54,7	Current at max power I_{mp} [A]	5,58
Temp. coefficient for V_{oc} [%/°C]	–0,273	Temp. coefficient for I_{sc} [%/°C]	0,062

In the PV array block setting, the PV panels were connected to a field containing 66 parallel strings that serve 5 modules in series. The PV array has 2 inputs. The first input is the solar radiation reported in watts per m^2 [W·m^{-2}], the second input is the temperature of the cell of the PV panel reported in Celsius degrees [°C]. The output of the PV array is a DC voltage and a measuring port *m* which contains the voltage and current of the PV cell, the diode current, the solar radiation and the temperature of the PV panel. Sunlight and solar panel temperature data were retrieved from the text file into the program. In Fig. 3 shows the I-V and P-V characteristics for the proposed PV array, under the solar radiation at three different intensities: 1000 W·m^{-2}, 500 W·m^{-2} and 100 W·m^{-2} when the PV panel temperature is constant $\vartheta = 25$ °C.

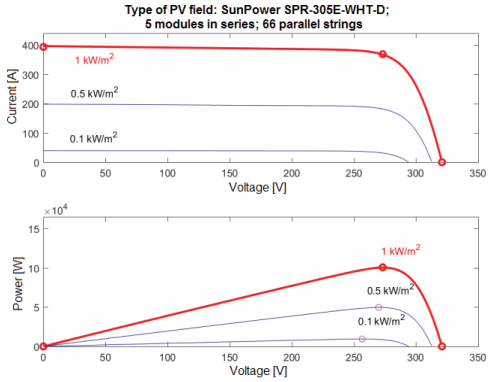

Figure 3. I-V and P-V characteristics for PV field at different solar radiation

Power output from the photovoltaic field is shown in Fig. 4. The DC current, which is generated by the PV panels, is controlled by a DC-DC amplifier, to which the MPPT controller operates. Subsequently, the current is changed to alternating current in a controlled three-phase VSC rectifier, including the inverter choke *RL*, the capacitive filter *C*, and the transformer TR1. The power is transferred out through a three-phase switch that is in the basic position "on". Block RL2 represents the power line by which is the PV field linked with the network. This model has been adapted and modified for the needs of this paper from MathWorks examples [8], [9].

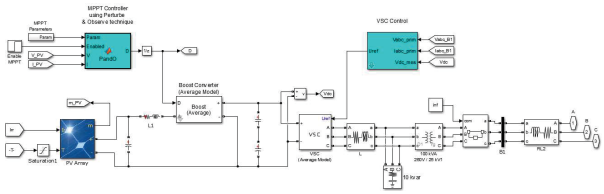

Figure 4. Power output from photovoltaic panels

C. *Wind turbine*

The wind turbine block with power-out transmission to the grid is considerably easier than a block of PV field. The wind turbine input is the *wind speed* reported in m·s^{-1} and a *Trip connector*. The wind speed for this model was retrieved from a text file. Trip connector serves to simulate the turbine protection system. Its input may be a logical zero or one. If at input is logical zero, the wind turbine is in operation and when at input is logical one, the turbine is disconnected. The wind turbine can have several protections. First of all, it is a wind turbine disconnection when there is slow/fast wind, but also overcurrent protection, undervoltage protection, overvoltage protection, or protection, acting in the unbalanced current or voltage.

The wind turbine output is a measuring port that contains the voltage and current at turbine terminals A, B and C, turbine output *P* and *Q*, turbine rotor speed, mechanical torque, and so on. The wind turbine used in this paper includes, in addition to the turbine, also an asynchronous engine that generates the

electrical energy. In Fig 5 is shown the characteristic output of the designed turbine at different wind speeds.

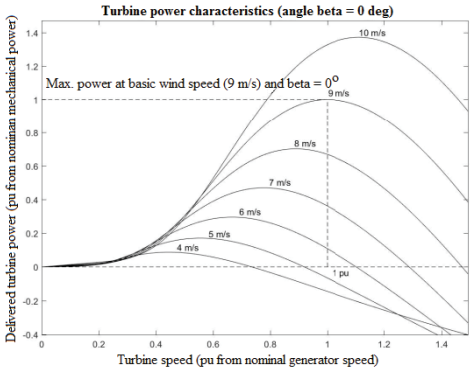

Figure 5. Characteristic turbine power at different wind speeds

Since during the simulation the disconnection of the wind turbine caused a mathematical error, the block "*Check static range*" was added to the scheme. This block stops the simulation if a wind speed is read at a speed that is not in the work range, and Matlab shows error message. The wind turbine operating range is in ranges from 4.5 $m \cdot s^{-1}$ to 12.5 $m \cdot s^{-1}$. The basic wind speed for the model turbine is 9 $m \cdot s^{-1}$.

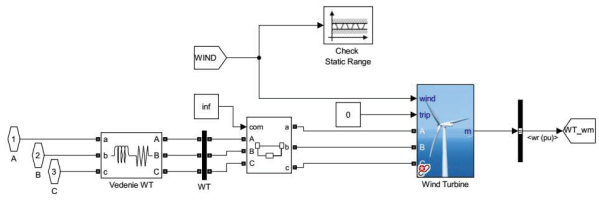

Figure 6. Wind turbine block with power delivery to the system

D. *Loads*

Simscape Power Systems offers several types of load. In this paper, three-phase serial *RLC* load and three-phase dynamic load were used. For both loads, the combined nominal voltage and nominal frequency of the network were entered.

For a static three-phase load, *PQ* power was input, which may be the same or specific for each load in all three phases. A static three-phase load contains also a voltage and current measurement that is optional [3], [4], [6].

For dynamic three-phase load, the *PQ* power was entered at the beginning of the simulation. The *PQ* power of a dynamic load can be controlled by an internal control that controls the amount of dynamic load based on the positive-sequence voltage component. If external control of power source is used, performance can be read from a file, and controlled by an external handling. The dynamic load contains also a measuring terminal *m*, the output of which is a vector with a positive-sequence voltage component, an active power *P* and a reactive power *Q* [5], [10].

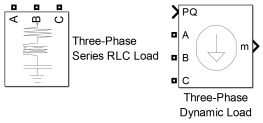

Figure 7. Loads in Simscape Power Systems

The loads were read using a Matlab script. In Fig 8, a proposed load block for the supply point A is shown. On the left, the load A1 and line A2 are shown, which are connected to the system via a three-phase circuit breaker and a power line simulated by the impedance R_a and L_a. Line A2 consists of a purely ohmical load, because the dynamic load line A1 cannot be connected in series with the inductive element of the three-phase line, which is the supply point connected to the system. On the right, the reading of block of line load A1 is displayed. If *init_const* = 1, the load, i.e. line A1 is set according to the vector from a text document. If *init_const* = 0, the load is set to the constant value, which is set in the text document for time $t = 0$. Current and voltage measurements were performed on bus-bar A. During the simulations, four consumption points A, B, C and D were considered. Each of these consumption points represents a part of the network. In some simulations, only static three-phase consumption points were used that were disconnected by a three-phase switch.

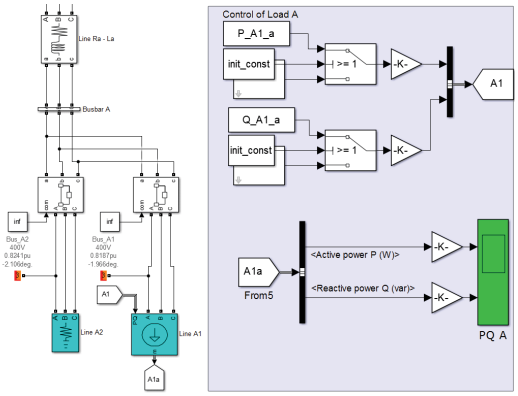

Figure 8. Designed load block with control

E. *Measurement in Simscape Power Systems*

In the simulations, electrical quantities were measured at selected locations in the network. Phase currents and voltages were measured using three-phase V-I measuring blocks, which were placed before loads and before the generators, resp. other sources. The measured output is the sinusoidal voltage/current depending on the time that has to be converted to the effective value (for comparison purposes). The scheme for measuring of the particular variables at the output of the G1 generator is shown in Fig. 9. The RMS current and voltage values for the L1 phase and the active and reactive power in the L1 phase were calculated from the measured currents and voltages.

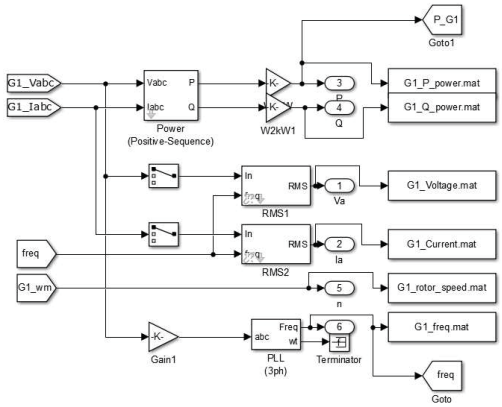

Figure 9. Scheme for control and measuring of monitored quantities

III. Mathematical Calculation of Off-Grid Network

A. *Model of a steady-state off-grid network*

In the off-grid steady-state model, the main aim was to point out that if no changes were made to the scheme and the correct initialization conditions were set, the network's frequency did not change and was 50 Hz. The phase voltage in phase L1 is equal to the portion of the line-to-line voltage and the square root of 3. If in a system were also considered losses on the line, the resulting voltage values were less than the expected 230 V. In the system were considered large losses on lines, so the phase voltages at the terminals were lower, namely: $U_{a\_A} = 220.5$ V, $U_{a\_B} = 221$ V, $U_{a\_C} = 223.1$ V, and $U_{a\_D} = 227$ V. The demand current depends on the size of the load being connected at the consumption point (load). The active and reactive *PQ* load was unchanged in the circuit.

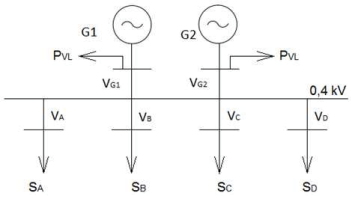

Figure 10. The steady-state model diagram

Table 3. Consumptions for Simulation of Steady-State Off-Grid Network

	U [V]	Demand power	Power factor cos φ	Overhead line	
				R [Ω]	L [μH]
G1, Self-consumption	400	12,5 kW	1	0,0025	11,27
G2, Self-consumption	400	12,5 kW	1	0,0025	11,27
Load A	400	100 kVA	0,95	0,0402	71,1
Load B	400	140 kVA	0,95	0,0268	47,4
Load C	400	180 kVA	0,95	0,0134	23,7
Load D	400	0	0,95	0,067	118,5

B. *Model of off-grid network with dynamic load*

In this part of the simulation there was modified model of loads. Instead of the loads modeled by the constant value, dynamic loads were used that were controlled by external input. Dynamic load operation is described in the previous chapter in part D. During these simulations, two generators with a nominal power of 250 kVA and four loads A, B, C and D were used in which the phase voltage and current in phase L1 and power value in L1 were measured.

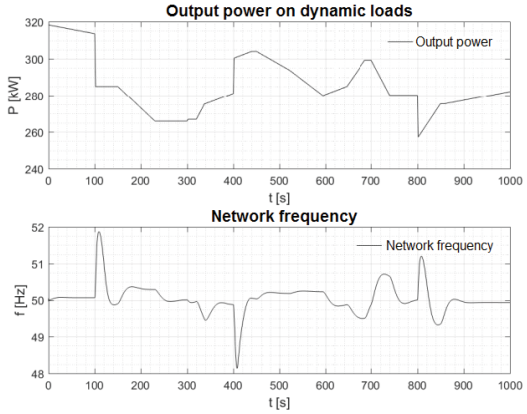

Figure 11. Network frequency response to output power

In Fig. 11, the abstraction performance is indicated by dynamic loads. Self-consumptions (2×12.5 kW) and parasitic loads to dynamic loads (3×9.5 kW + 4.75 kW), which are purely resistive, have to be added to the total output power. These parasitic loads are in the system because dynamic loads and synchronous generators cannot be in series with an inductive element of three-phase power lines. Those are described by the *RL* parameters listed in Tab. IV.

Table 4. Resistance and Inductance of Power Lines in Simulations with Dynamic Load

	R [Ω]	L [μH]
G1	0,0025	11,27
G2	0,0025	11,27
A	0,2010	355,50
B	0,0268	47,40
C	0,0134	23,70
D	0,0670	118,50
PV	0,0099	45,10
WT	0,0099	45,10

By a continual decreasing, respectively by increasing of the power consumption there has been observed, that the regulators of the synchronous generators respond to these changes, and there is a decrease, respectively increase in output power produced by synchronous generators, but the frequency is not regulated to the nominal value of $f_n = 50$ Hz. Thus, the frequency of the network will be short-lived at a different value near the nominal frequency due to the rate of decrease/increase of the consumed power. This can also be seen in Fig. 11, from 478 seconds to 595 seconds, the network's frequency was around 50.2 Hz. From 900 s to 1000 s the network frequency was stable at values between 49.93 and 49.95 Hz.

C. *Off-grid network model with photovoltaic field*

In the world, there is a tendency for off-grid networks that are powered by diesel generators to install renewable energy sources to reduce diesel consumption in diesel generators. In the mentioned model, photovoltaic panels with a total peak power of 100 kW were connected to the simulated off-grid network.

The Fig. 12 shows the solar radiation captured onto the photovoltaic field depending on the simulation time. At the beginning of the simulation, i.e. at time $t = 0$ s, the solar radiation captured on the PV field, is 857.4993 W·m^{-2}. At time $t = 276$ s, solar radiation decreases to 266.2146 W·m^{-2}, which is the first minimum of tested sunlight. At time $t = 700$ s, a second low of 242.5764 W·m^{-2} solar radiation occurs. Both decreasing of solar radiation were due to increased cloud cover. The photovoltaic cell temperature was around 27 °C. These data were measured in August 2013 as a part of a hybrid photovoltaic system operated by the Department of Electrical Power Engineering, FEI TU in Košice. These data represent actual data under the conditions for which the electricity from the PV field was produced.

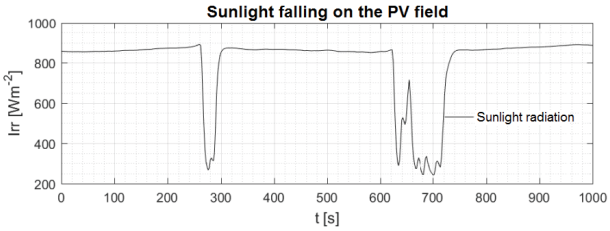

Figure 12. Sunlight falling on the PV field

B1. Off-grid network with PV-field and constant consumption

In order to best see the network's response to sudden drop in power output from the PV field, constant load values were set when simulating the photovoltaic field. In this case, the output produced by the diesel generators is adapted to the output produced by the PV field. The Fig 13 shows the PV field response to the test climatic conditions shown in Fig 11. At the same time, Fig 13 shows the response of generator no. 1. Generator no. 1 and 2 were connected in series, so generator 2 produces the same power as generator 1. So when the output of the PV field drops by 60 kW due to meteorological conditions, both generators must start to produce 30 kW more power.

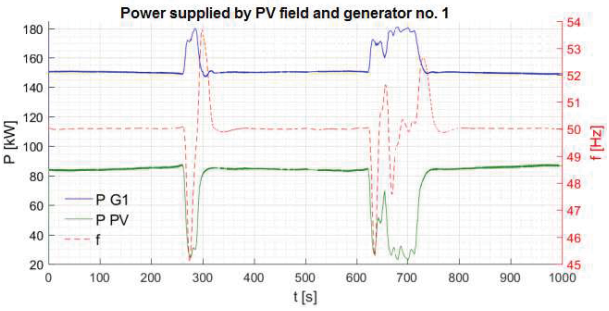

Figure 13. The frequency of the network and the power output of the PV array with the generator no. 1

This simulation shows that the PV field is capable of producing relatively high power, but due to the increased cloud, short-term power failures can occur in the PV field output. The off-grid network simulation was implemented without any added controllers that would run the network on the load side. If an off-grid network was operated in this way, it is likely that the quality and reliability of electricity would be limited. In the simulation, the network frequency dropped from 50 Hz to below 46 Hz. While diesel generators are capable of operating in a wide frequency range, a mentioned rapid drop in frequency would be at risk.

D. *Off-grid model with a wind turbine that operates at a dynamic wind speed*

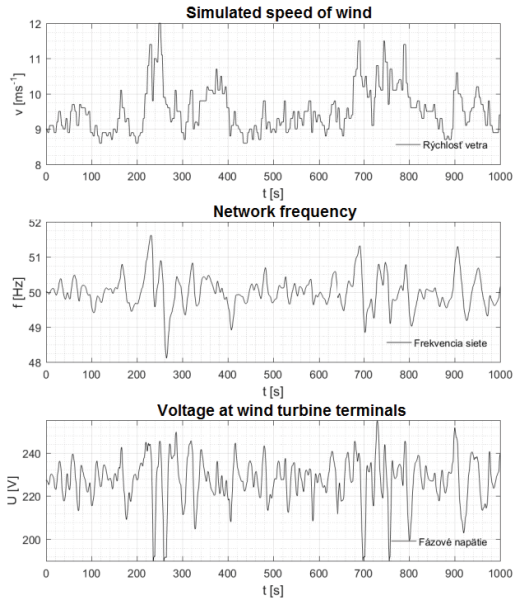

Figure 14. Simulated wind parameters

Wind simulation was used to simulate the wind-flow circuit as it is illustrated in Fig. 14. The wind loaded from the text file has a value of 9 m·s^{-1} at time $t = 0$, which is the nominal wind for the wind turbine used. Subsequently the wind varies around this value. Wind reaches a maximum value of 12 m·s^{-1}. The wind turbine operates with winds ranging from 4.5 m·s^{-1} to 12.5 m·s^{-1}.

Since the simulated wind turbine has no stabilizing mechanism, the supplied turbine power also varies around the nominal value. This was reflected negatively on network frequency and voltage. Since the simulated off-grid network is small in size, voltage fluctuations have been registered in all four A, B, C and D loads. Frequency of the grid and voltage at the wind turbine terminals are shown in Fig. 13. Referring to Fig 13 it can be seen that even with small wind changes, the frequency has risen above 51 Hz, or falls below 49 Hz. Voltage at wind turbine terminals is fluctuating. In case of a sudden change of wind, the voltage exceeds 250 V, respectively drops to 190 V. Since the voltage fluctuations are relatively strong, a digital flickermeter has been connected to load points A, B, C and D and to the wind turbine connection point.

C1. Flicker-effect measure in network with a wind turbine

In the previous section C there was a description of off-grid operation with a wind turbine with dynamic wind. In order to determine the flicker effect in the aforementioned network, a digital flickermeter was added at points A, B, C and D to find a short-term flicker rate that is calculated at simulation time of 5 to 605 s, representing a ten minute time period. In tab. V is the measured short-term rate of flicker and averaged percentiles. The smallest rate of flicker short-term perceptive was simulated with a constant wind velocity of 9 m·s^{-1} and a dynamic load. On the other side, the highest short-term flicker rate was simulated with dynamic wind speed and dynamic load. The limiting value for the short-term flicker was 1, for a long-term flicker value (for 2 hours) of 0.65. From the measured results it can be stated that the short-term flicker rate was in accordance with standard STN EN 50160.

The Fig 15 shows the measured instantaneous level of the flicker effect at the load point C for dynamic load simulation (Fig. 11) and the dynamic wind simulation (Fig. 14). From Fig. 15, it is apparent that the blink effect was occurred in the case of dynamic load simulation at a time when the load was connected or disconnected in the network. It was observed for example, at time $t_1 = 100$ s when a load of 30 kVA was disconnected at the load point B or at time $t_2 = 400$ s when a load of 20 kVA was connected at the load point C or at time $t_3 = 800$ s when the load of 20 kVA was disconnected from load point C. In the case when the dynamic wind acts on the wind turbine (see Fig. 14), the measured instantaneous level of flicker effect will appear as stochastic noise.

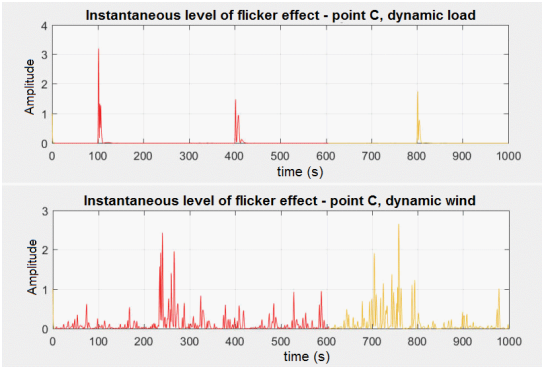

Figure 15. Measured instantaneous level of flicker effect

The Tab. V shows the short-term flicker rate response for the load points A, B, C and D and for the point on the wind turbine terminals. The particularity of these results is that in each simulated scheme, at the load point A, the highest degree of short-term flicker is measured. This is due to the fact that the point A is powered by a line whose resistance and reactance is much larger than the lines connecting the other points (see Tab. IV). The voltage at point A in these simulations was stabilized at $U = 189.6$ V (in real conditions, such a low voltage would be a problem for the operation of many devices).

Table 5. Flicker Effect in the Simulated Network

		$P_{0.1s}$	P_{1s}	P_{3s}	P_{10s}	P_{50s}	P_{st}
Simulation with WT, dynamic wind speed, dynamic load	Point A	7,94444	2,29646	1,09671	0,364422	0,043251	0,739981
	Point B	4,42942	1,38709	0,654338	0,225327	0,025813	0,565732
	Point C	4,12629	1,33554	0,640592	0,221686	0,025551	0,553068
	Point D	4,28825	1,38515	0,663718	0,22959	0,026457	0,563365
	Pt. WT	3,90262	1,27304	0,611244	0,212224	0,024508	0,539369
Simulation with WT, dynamic wind speed, constant load	Point A	4,76669	2,50239	1,21876	0,547187	0,068989	0,721009
	Point B	2,29082	1,2644	0,642569	0,286289	0,037393	0,5135
	Point C	2,18987	1,20936	0,615162	0,273998	0,035838	0,502251
	Point D	2,27869	1,25794	0,63941	0,284875	0,03721	0,512195
	Pt. WT	2,09109	1,15719	0,590026	0,262503	0,034409	0,491356
Simulation with WT, constant wind speed, dynamic load	Point A	4,96686	1,67448	0,38066	0,014602	0,011166	0,523317
	Point B	3,04421	0,966101	0,218407	0,00848	0,006955	0,404461
	Point C	2,77123	0,929307	0,212038	0,007767	0,00631	0,390405
	Point D	2,87724	0,959631	0,21867	0,008057	0,006548	0,397332
	Pt. WT	2,64433	0,879365	0,199992	0,007509	0,006025	0,380651

In order to reduce the influence of power line on the measured flicker effect, the simulations were repeated except that the line joining the load point A was simulated by resistance $R_c = 0.0134\ \Omega$ and inductance $L_c = 23.7\ \mu H$ connecting the load point C. The results are given in Fig. 16.

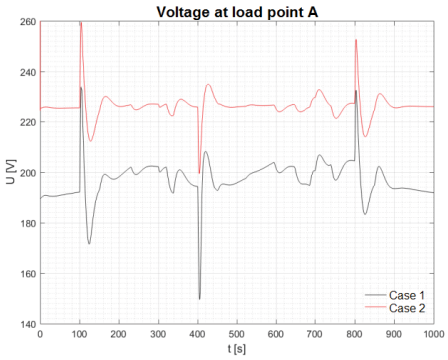

Figure 16. Voltage in simulated scheme for point A

In Fig. 16 is the voltage characteristics at the load point A in the case where was considered constant wind of 9 m·s^{-1} during the whole simulation and the dynamic load as described in section B. For the case 1 there was considered the original power line whose resistance was $R_a = 0.2010\ \Omega$ and inductance $L_a = 355.5\ \mu H$. In case 2, a point A was connected by a line with parameters $R_a = 0.0134\ \Omega$ and $L_a = 23.7\ \mu H$.

From Fig. 16, it is clear that in case 1 there is a greater voltage fluctuation at the terminals at the load point A as in case 2. For example, during the disconnection of the 20 kVA load from the load point C, there was observed (in case 1) at the load point A the short-term voltage drop from $U_f = 194.3$ V to $U_f = 149.5$ V, which is a drop of $\Delta U = 44.8$ V. In case 2, there was drop from $U_f = 225.7$ V to $U_f = 199.4$ V, which is drop of $\Delta U = 26.3$ V. As there is less voltage fluctuation in transient phenomena, the resulting flicker effect will be less. In test example 2, the value of the Short Term Perceptibility (P_{st}) of flicker effect in point A was $P_{st} = 0.335491$ (the original value, in case A was $P_{st} = 0.523317$).

IV. Conclusion

This paper presented the results of off-grid network simulations with consideration of renewable resources (PV source and wind turbine) and without considering RES. The simulated off-grid network consisted of two diesel generators with a nominal output of 250 kW and with loads A, B, C and D, representing 4 load points representing 4 off-grid sites. In the case of a load disconnection or connection, the generators are able to regulate the system so that the power output is equal to the power delivered. The regulation of diesel generators has ensured the control of the hydraulic turbine.

The problem of off-grid systems with a photovoltaic field is that the power output from the PV field cannot be regulated. The PV field produces electricity according to current climatic conditions. Therefore, in the case of rapid climate change, there is a rapid change in the output of the PV field. For example, with increased cloudiness, a sudden drop in the electricity produced from the PV field may occur. By adding a wind turbine into an off-grid, an increased flicker effect was observed. In addition to voltage fluctuations in the network, the network frequency also varies. Large frequency fluctuations can have a negative impact on diesel generators. Flicker effect occurs when disconnecting or connecting loads, resources, and off-grid networks. In both cases, it is necessary to consider how to remove the unfavorable phenomenon of blinking.

Acknowledgement

This work was supported by the Ministry of Education, Science, Research and Sport of the SR and the Slovak Academy of Sciences under the contract No. VEGA 1/0132/15.

References

[1] Z. Čonka, "Impact of renewable energy sources on stability of EWIS transmision system", In: *proc. 14th Int. Conf. on Env. and El. En.:* Krakow, Poland, 10-12 May, 2014. Danvers: IEEE, 2014 P. 75-79. ISBN 978-1-4799-4661-7.

[2] R. Cimbala, L. Kruželák, S. Bucko, J. Kurimský, M. Kosterec, "Influence of Electromagnetic Interference on Time-Domain Spectroscopy of Magnetic Nanofluids", In: *EPE 2016.* Danvers: IEEE, 2016, p. 279 - 282. ISBN 978-1-5090-0907-7.

[3] M. Pavlík, "Prediction of electricity price using RSI mechanism", In: *Scientific Letters of Academic Society of M. Baludansky*, Vol. 4, No. 6A (2016), p. 82-84. ISSN 1338-9432.

[4] J. Zbojovský, P. Liptai, M. Moravec, "Modelling and calculating the shielding effectiveness of building materials", In: *Technical sciences and technologies*. Vol. 6, no. 4 pp. 205-210. ISSN 2411-5363, 2016

[5] M. Kanálik, M. Pavlík, M. Kolcun, "The impact of multi-system overhead lines operation with different voltage levels to voltage unbalance", In: *Elektroenergetika 2015.* Košice: TU, pp. 73-76. ISBN 978-80-553-2187-5, 2015

[6] M. Kanálik, M. Kolcun, "Computation of harmonic flows in three-phase systems". In: *Acta Electrotechnica et Informatica.* Vol. 7, No. 3, pp. 41-45. ISSN 1335-8243, 2007

[7] MathWorks, "*Model hydraulic turbine and proportional-integral-derivative*", < https://www.mathworks.com/help/physmod/sps/powersys/ref/hydraulicturbineandgovernor.html >

[8] MathWorks, "*Three-Level Bridge*", < https://www.mathworks.com/help/physmod/sps/powersys/ref/threelevelbridge.html >.

[9] MathWorks, "*Average Model of a 100-kW Grid-Connected PV Array*",<https://www.mathworks.com/help/physmod/sps/examples/average-model-of-a-100-kw-grid-connected-pv-array.html >

[10] MathWorks, *"Implement three-phase dynamic load with active power and reactive power as function of voltage or controlled from external input"*, < https://www.mathworks.com/help/physmod/sps/powersys/ref/threephasedynamicload.html >..